DOI: 10.6060/mhc234971m

Advances in Tetrapyrrolic Chemistry over 2018-2022 of Research Group Headed by Full Member of RAS A. Yu. Tsivadze: Highlights on the Occasion of his Anniversary

Alexander G. Martynov,[a@] and Yulia G. Gorbunova[a,b@]

[a]*Frumkin Institute of Physical Chemistry and Electrochemistry RAS, 119071 Moscow, Russia*
[b]*Kurnakov Institute of General and Inorganic Chemistry RAS, 119991 Moscow, Russia*
[@]*Corresponding author E-mail: martynov@phyche.ac.ru, yulia@igic.ras.ru*

This brief review summarizes and highlights some of scientific advances in the field of porphyrin/phthalocyanine chemistry, which were achieved under the leadership of Full member of Russian Academy of Sciences, Professor Aslan Tsivadze over 2018–2022.

Keywords: Porphyrins, phthalocyanines, supramolecular chemistry, photophysics, biomedical applications, catalysis, magnetic materials, molecular switchers.

Обзор достижений в области химии тетрапиррольных соединений, полученных в группе академика А. Ю. Цивадзе за период 2018-2022 гг.

А. Г. Мартынов,[a@] Ю. Г. Горбунова[a,b@]

[a]*Институт физической химии и электрохимии им. А.Н. Фрумкина РАН, 119071 Москва, Россия*
[b]*Институт общей и неорганической химии им. Н.С. Курнакова РАН, 119991 Москва, Россия*
[@]*E-mail: martynov@phyche.ac.ru, yulia@igic.ras.ru*

В кратком обзоре приведены достижения в области химии тетрапиррольных соединений, полученные в группе академика РАН А.Ю. Цивадзе за период 2018–2022 гг.

Ключевые слова: Порфирины, фталоцианины, супрамолекулярная химия, фотофизика, биомедицинские приложения, катализ, магнитные материалы, молекулярные переключатели.

Dear Readers! This issue of the “Macroheterocycles” contains several papers dedicated to Professor Aslan Yusupovich Tsivadze, full member of Russian Academy of Sciences, President of Mendeleev Russian Chemical Society, scientific leader of A.N. Frumkin Institute of Physical Chemistry and electrochemistry of Russian Academy of Sciences on the occasion of his 80 birthday.

This welcoming review summarizes and highlights some of scientific advances in the field of tetrapyrroles, which were achieved under the leadership of A. Yu. Tsivadze over 2018–2022. This digest complements a previous review published five years ago.[1]

Recent selected results will be presented in following interconnected fields:

- *Synthesis of novel macrocyclic systems*
- *Spectroscopy and theory*
- *Biomedical applications*
- *Catalytic applications*
- *Hybrid materials*
- *Proton-conducting metal-organic frameworks*
- *Magnetic materials*
- *Molecular switches and supramolecular chemistry*

Synthesis of Novel Macroheterocyclic Systems

In the last five years, special attention has been paid to the development of synthetic approaches to extended analogues of porphyrins and phthalocyanines. It is known that such an extension changes the physicochemical properties of macrocycles, which is widely used to tune their functional characteristics.

Porphyrins conjugated with heterocycles

A general strategy for the preparation of functionalized imidazole- and pyrazine-appended porphyrins involving *in situ* generation of 2,3-diaminoporphyrin and its subsequent interaction with carbonyl compounds was developed (Figure 1).[2]

Several methods for the post-synthetic modification of imidazo[4,5-]porphyrins were also proposed. First, a synthetic approach to the isomeric difunctionalized porphyrins, containing two β,β′-fused 2-aryl-1-imidazole cycles at adjacent or opposite pyrrole rings of the macrocycle was developed. The core chemistry of this synthetic route was the transformation of 2-aryl-1-imidazo[4,5-]porphyrins into corresponding imidazodioxochlorins followed by Debus–Radziszewski condensation with aromatic aldehyde. Next, 2-(4-bromophenyl)-1-imidazo[4,5-]-5,10,15,20-tetramesitylporphyrin was transformed into useful carboxy- and phosphonato-substituted precursors for material chemistry according to palladium-catalyzed C–C and C–P bond forming reactions.[3,4]

A convenient synthetic strategy for the efficient preparation of new functionalized low-symmetry A_2BC-type porphyrins bearing *meso*-areneimidazolyl fragment was developed. The reactivity of the key precursors, namely 5-bromo-15-imidazolylporphyrins, in C–C-coupling reactions was evaluated providing access to target functional derivatives.[5]

Heteroleptic sandwich complexes with imidazole- or pyrazine-appended low-symmetry porphyrin ligands were synthesized, and influence of heterolcyclic annelation on optical properties of complexes was revealed.[6]

Zinc complex with 2-(4-pyridyl)-1H-imidazo[4,5-b]porphyrin was found to behave as a supramolecular tecton: in crystalline phase, this complex exists as a zigzag coordination polymer formed through the axial coordination of the pyridine nitrogen atom to the zinc ion of the neighbouring porphyrin molecule.[7]

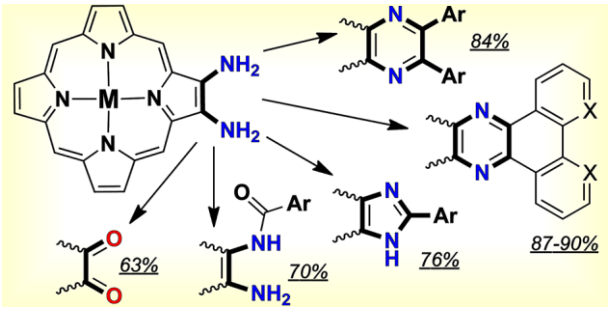

Figure 1. Revisiting 2, 3-diaminoporphyrins: key synthons for heterocycle-appended porphyrins.[2]

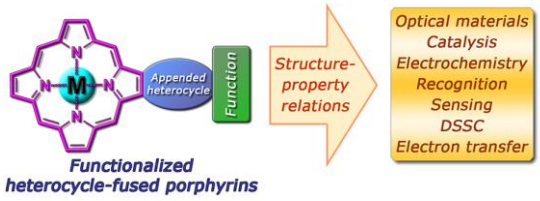

Figure 2. Heterocycle-appended porphyrins: synthesis and challenges.[9]

New pyrazine-fused porphyrin dimer was unexpectedly produced by mild oxidation of [2,3-diamino-5,10,15,20-tetrakis(4-butoxyphenyl)porphyrinato]nickel(II) in 40% yield. The obtained porphyrin dimer demonstrated bathochromic shift of absorption bands compared to the reported analogues, along with panchromatic absorption in the 250–650 nm range, which is promising for optical, photovoltaic and medical applications.[8]

The advances in synthesis of heterocycle-appended porphyrins were summarized in a comprehensive review,[9] which also comprises the most interesting and promising physical-chemical properties of these compounds and related challenges of their practical applications in different fields (Figure 2).

π-Extended derivatives of phthalocyanines

Tetra-15-crown-5-naphthalocyanines as first representatives of crown-substituted π-extended phthalocyanines were synthesized and characterized (Figure 3). The possibility to control their aggregation and photophysical properties by reversible formation of supramolecular assemblies in the presence of KOAc was demonstrated.[10] In course of investigation of crown-substituted phthalo- and naphthalocyanines the side process of aromatic nucleophilic substitution causing crown-ether cleavage was found.[11] The guidelines were suggested for the choice of bases and template agents in the synthesis of (na)phthalocyanines functionalized with macrocycles.

The approach toward synthesis of 5,8-disubstituted naphthalonitriles as the universal platform for the range of novel functionalized highly soluble and nonaggregating naphthalocyanines was developed.[12] The selective bromination of 15-crown-5-naphthalonitrile was described, that can pave way to wide application of transition-metal catalyzed cross-coupling reactions for the synthesis of functionalized naphthalonitriles and naphthalocyanines based on 6,7-dialkoxy-substituted precursors.

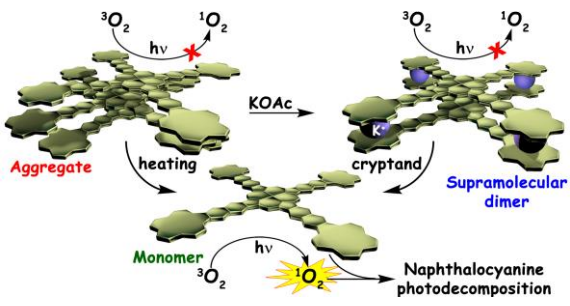

Figure 3. Crown-substituted naphthalocyanines: synthesis and supramolecular control over aggregation and photophysical properties.[10]

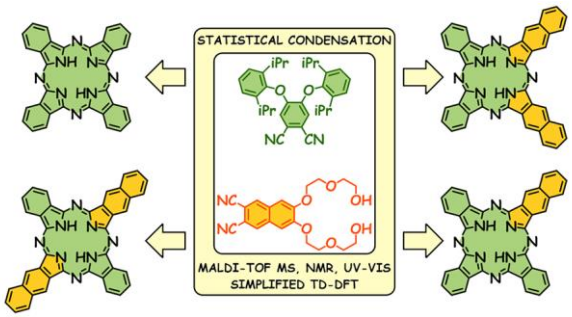

Figure 4. Synthesis, electronic structure and NH-tautomerism of novel mono-and dibenzoannelated phthalocyanines.[13]

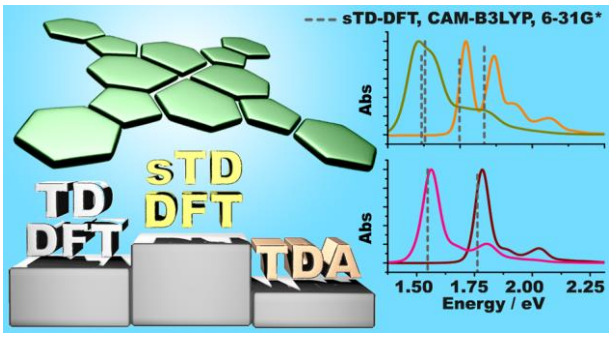

Figure 5. Methodological survey of simplified TD-DFT methods for fast and accurate interpretation of UV–vis–NIR spectra of phthalocyanines.[15]

Novel low-symmetry benzoannelated metal-free phthalocyanines of A_3B-, ABAB- and AABB-types were synthesized by statistical condensation of phthalonitrile A bearing bulky solubilizing groups and new naphthalonitrile B with OH-terminated diethylene glycol anchors (Figure 4).[13] Comprehensive physical-chemical characterization of the synthesized macrocycles allowed to identify the spectroscopic signatures of various tautomers including energy-unfavourable forms and provided tools to control their aggregation.[14]

Spectroscopy and Theory

A methodological survey of density functional theory (DFT) methods for the prediction of UV–visible–near-infrared spectra of phthalocyanines was reported.[15] Four methods, namely, full time-dependent TD-DFT and its Tamm–Dancoff approximation (TDA), together with their simplified modifications (sTD-DFT and sTDA, respectively), were tested by using the examples of unsubstituted and alkoxy- substituted metal-free ligands and zinc complexes (Figure 5). The theoretical results were compared with experimental data derived from UV–visible absorption and magnetic circular dichroism spectroscopy. This work was performed with the colleagues from Rhodes University (Prof. Tebello Nyokong group, South Africa).

The best accuracy for the gas-phase vertical excitations was observed in the lower-energy Q-band region for calculations that made use of range-separated hybrids for both full and simplified TD-DFT approaches. The CAM-B3LYP functional provided particularly accurate results in the context of the sTD-DFT approach. Together with a general increase in accuracy, the application of simplified TD-DFT methods affords a 2–3 orders of magnitude speedup of the calculations in comparison to the full TD-DFT approach. Thus this method can be readily used on desktop computers during the interpretation of UV–Vis–NIR spectra of phthalocyanines and related macrocycles, and numerous examples of its successful application were reported by our group over last five years.[12,13,16–19]

DFT calculations were also widely used to explain various phenomena related to tetrapyrrole reactivity and spectroscopy, including formation and photophysics of complexes with phosphorus(V),[20,21] nucleophilic substitution of bromine in β-bromo-porphyrins,[22] optical limiting by In(III) and Ga(III) complexes with low-symmetry phthalocyanines,[23] conjugation in imidazoporphyrins with appended polycyclic aromatic hydrocarbons,[24] Raman spectroscopy of phthalocyanines for development of ultra-sensitive optical fingerprinting of biorelevant molecules on nanostructured metasurfaces.[25]

Biomedical Applications

Novel photosensitizers and multimodal agents for thermometry and imaging

New synthetic pathway toward water-soluble phthalocyanines bearing cationic 4-(N,N,N-trialkylammonium-methyl)-phenoxy groups has been elaborated (Figure 6).[26] It involved the convenient reductive amination of various (4-formylphenoxy)-substituted phthalonitriles with diethylamine and $NaBH(OAc)_3$, leading to 3-, 4- and 4,5-(p-diethylaminomethyl-phenoxy)-substituted phthalonitriles as precursors to new Zn(II), Mg(II) and metal-free phthalocyanines containing four or eight cationic groups in non-peripheral (α-) or peripheral (β-) positions. Cationic complexes showed moderate solubility in water with high tendency to aggregation, however α-substituted Zn(II) and Mg(II) complexes existed in water in predominantly monomeric states capable of singlet oxygen generation. Further monomerization of Zn(II) complex in aqueous solution was achieved by interaction either with non-ionic surfactant Tween-80 or bovine serum albumin (BSA). The advantage of these results was not limited to new convenient synthetic approach to the cationic phthalocyanines but it also consisted in preparation of new phototherapeutic agents with promising photophysical and photochemical properties.

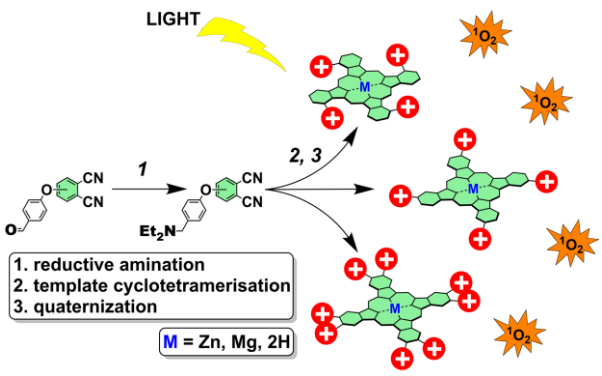

Figure 6. Robust route toward cationic phthalocyanines through reductive amination.[26]

Anti-cancer treatment efficiency can be significantly enhanced by the synergistic effect of the combined phototherapy that nowadays is under intensive preclinical and clinical studies. To minimize collateral damage, the combined phototherapy should be accompanied by a real-time thermal sensing. However, it is still challenging to develop multifunctional agent which combines therapy and temperature control.

In collaboration with Saint Petersburg State University we have shown that contactless fluorescent thermometry based on ratiometric and lifetime approaches can be performed using water-soluble anionic tetra sodium salt of *meso*-tetrasulfonatophenylporphyrinate and cationic *meso*-mono(4-pyridyl)-triphenylporphyrinatophosphorus(V) bromide MPyPP(OH)$_2$ photosensitizers (Figure 7).[27] Both sensing techniques provide simple linear calibration curves in the biological temperature range. Porphyrins' cytotoxicity was studied in vitro both in dark and blue-light activated conditions. Exposure-dependent cell viability showed that porphyrins could be used as molecular thermometers for phototherapy to avoid heat-induced adverse effects or as promising photosensitizers depending on chosen laser power.

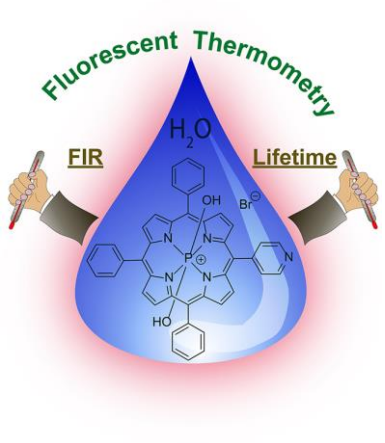

Figure 7. Water-soluble multimode fluorescent thermometers based on porphyrins photosensitizers.[27]

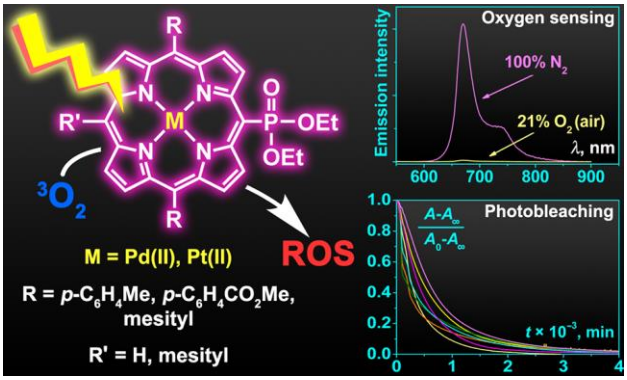

Figure 8. Platinum(II) and palladium(II) complexes with electron-deficient meso-diethoxyphosphorylporphyrins: synthesis, structure and tuning of photophysical properties by varying peripheral substituents.[29]

MPyPP(OH)$_2$ was then used as subcellular ratiometric thermal sensor in CHO-K1 and HeLa cells within the biological temperature range (30–44 ºC).[28] Introduction of porphyrin into cells resulted in its dephosphorylation and change of luminescence properties. Ratiometric sensing was performed using peak-to-peak and peak-to-valley ratios. Thermometric performance was evaluated in terms of absolute and relative sensitivities, temperature resolution. Relative thermal sensitivity and temperature resolution reached 0.61% K^{-1} and 0.1 ºC, respectively in the case of CHO-K1 cells.

A series of electron-deficient platinum(II) and palladium(II) complexes with phosphorylated porphyrins was synthesized and it was demonstrated that these complexes emit at room temperature in the near-infrared region at 670–770 nm (Figure 8).[29] Effective homogeneous oxygen quenching and good sensitivity in toluene (~155 Pa^{-1} s^{-1}) were observed for the platinum(II) complexes with phosphorylporphyrins in solution. Platinum and palladium trimesitylphosphorylporphyrins exhibit high photostability in DMF solution and seem to be the most potentially interesting derivatives of the series for oxygen sensing in biological samples and the covalent immobilization on solid supports to prepare sensing devices including optic fibers. This study was performed in collaboration with colleagues from Institute of Analytical Chemistry and Food Chemistry, Graz University of Technology, Austria (Dr. Sergey M. Borisov) and Institut de Chimie Moléculaire de l'Université de Bourgogne, Dijon, France (Dr. Alla Bessmertnykh-Lemeune).

Binding of photosensitizers with bilayer lipid membranes

Bilayer lipid membranes (BLM) have already been widely acknowledged as convenient models to study binding of photosensitizers with cell surfaces and mimic photodynamic action in membrane environment.[30] In collaboration with the laboratory of bioelectrochemistry (IPCE RAS) we reported the synthesis, lipid membrane binding and photodynamic activity of three novel cationic PSs based on β-imidazolyl-substituted porphyrin and its Zn(II) and In(III) complexes.[31] Comparison of the behavior of the investigated porphyrins at the BLM demonstrated the highest adsorption for the In(III) complex and the lowest one for Zn(II) complex. The photodynamic efficiency of these porphyrins was evaluated by determining the oxidation rate of the styryl dye, di-4-ANEPPS, incorporated into the lipid membrane. These rates were proportional to the surface density of the porphyrin molecules at the BLM and were roughly the same for all three porphyrins. This indicates that the adsorption of these porphyrins at the BLM determines their photodynamic efficiency rather than the extinction or quantum yield of singlet oxygen.

We also reported the synthesis, membrane binding properties and photodynamic efficiency of novel dicationic free-base, Ni(II) and Zn(II) pyrazinoporphyrins with terminal tetraalkylammonium groups, to show the possibility to enhance the membrane binding of PS molecules, regardless of the central cation (Figure 9).[32] All of these substances adsorb at the lipid membrane, while free-base and Zn(II) porphyrins actively generate singlet oxygen in the membranes. Thus, this study revealed a new way to tune the PDT activity of PSs in biological membranes through de-

signing the structure of the peripheral groups in the macrocyclic photosensitizer.

Hybrid materials for biomedical applications

The influence of cerium oxide nanoparticles on singlet oxygen generation upon photosensitizer irradiation was studied in collaboration with Laboratory of Synthesis of Functional Materials and Mineral Processing (IGIC RAS).[33] Thus, solutions of tetra-15-crown-5-phthalocyanines (aluminium(III), gallium(III) and indium(III) hydroxide) in DMSO were used as photosensitizers. Ceria nanoparticles (CNPs) were shown to inhibit the photobleaching process of the crown-phthalocyanines induced by UV- and visible irradiation of these photosensitizers. The photoprotective properties of CNPs were shown to depend on their size and lattice parameter, with these in turn being determined by conditions of CNPs' synthesis. In addition, the deactivation of the reactive oxygen species and the UV-shielding effect of ceria nanoparticles were demonstrated.

Association of photosensitizer molecules with nanoparticles that perform the delivery function can lead to a change in the functional state of the photosensitizer. Thus, in collaboration with Faculty of biology in Lomonosov Moscow state university we studied the effects observed upon incorporation of octa- and hexadeca-carboxyphthalocyanines of zinc(II) and aluminum(III) (Pcs) into the polymer shell of nanoparticles with a semiconductor CdSe/CdS/ZnS core with various spectral and optical methods.

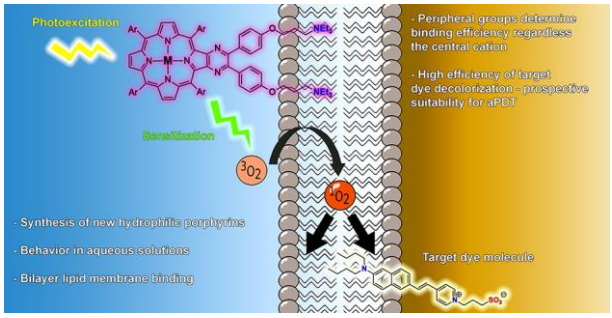

Figure 9. Lipid membrane adsorption determines photodynamic efficiency of pyrazinoporphyrins.[32]

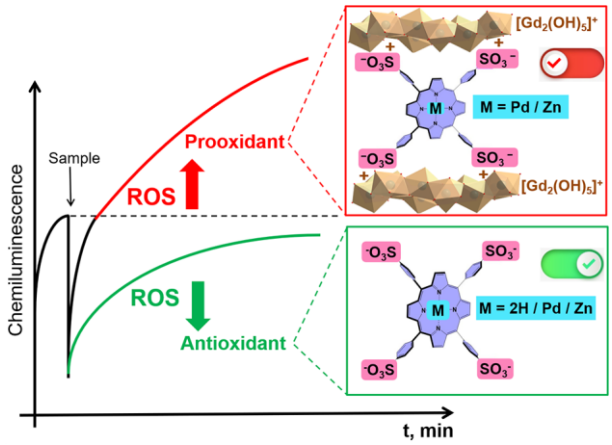

Figure 10. Switchable nanozyme activity of porphyrins intercalated in layered gadolinium hydroxide.[34]

First, the interaction of Pc with the polymer shell lead to a change in the spectral properties of Pc; the effect strongly depends on the structure of the Pc molecule (number of carboxyl groups as well as the nature of the central cation in the macrocycle). Secondly, upon incorporation of several Pc molecules, concentration effects became significant, leading to Pc aggregation and/or nonradiative energy transfer between neighboring Pc molecules within a single nanoparticle. These processes lead to the decrease of a number of the Pc molecules in an excited state. Such effects should be taken into account during the development of multifunctional platforms for the delivery of photosensitizers, including the use of nanoparticles as enhancers of photosensitizer activity by energy transfer.

Organo-inorganic nanohybrids with enzyme-like activity were prepared by in situ intercalation of anionic 5,10,15,20-tetrakis(4-sulfonatophenyl)porphyrin and its Zn(II) and Pd(II) complexes into gadolinium layered hydroxide.[34] The enzyme-like activity of individual constituents and hybrid materials, was studied by chemiluminescence analysis using the ABAP/luminol system in phosphate buffer solution (Figure 10). All the individual porphyrins exhibited dose-dependent antioxidant properties with respect to alkylperoxyl radicals at pH 7.4. The intercalation of free base porphyrin into the layered hydroxide preserved the radical scavenging properties of the product. Conversely, in hybrid samples containing Zn(II) and Pd(II) complexes, the antioxidant properties of the porphyrins changed to dose-dependent prooxidant activity. Thus, an efficient approach to the design and synthesis of advanced materials with switchable enzyme-like activity was developed.

Catalytic Applications

Photocatalysis

New promising photoactive functionalized pyrazinoporphyrins were prepared and preliminarily tested as homogeneous catalysts in the photooxidation of organic sulfides (Figure 11).[35] An extremely low loading of the catalysts (10^{-3} mol%) allowed oxidation of thioanizole to the corresponding sulfoxide with the conversion of 98–100%, TON *ca*. 95060–98000 and TOF *ca*. 5941–6125, providing the selectivity of the corresponding sulfoxide formation of 97–98%. A survey of the *meso*-substituents of the porphyrin was performed allowing determination of optimal derivatives providing high catalytic activity together with sufficient stability and solubility under reaction conditions and along the synthetic pathway. The presence of the diethoxyphosphoryl- and methoxycarbonyl-substituents in the prepared compounds allows to consider them as prospective starting materials for further grafting to solid supports and thus as a platform for the development of heterogeneous photocatalysts.

A series of π-expanded pyrazinoporphyrins were successfully prepared and tested as sensitizers for photocatalytic aerobic sulfides oxidation.[36] 2,3-Diaminoporphyrin derivative was used as a key intermediate for the preparation of porphyrins fused with naphtho-, phenanthrene-, phenanthroline- and acenaphthoquinone fragments. The photocatalytic performance of the obtained π-expanded pyrazinoporphyrins was investigated in the aerobic oxidation of thioanisole and revealed the increase of the activity with the ex-

pansion of the π-system of the molecule. The maximal TON = 89,000 could be reached with 10^{-3} mol% catalyst loading. DFT analysis revealed the presence of orbitals with predominant localization either at porphyrin macrocycle or at peripheral polyaromatic part of the molecule, allowing to expect charge separation upon photoexcitation.

Phthalocyanines as catalysts in carbene transfer reactions

Catalytic activity of iron and ruthenium phthalocyaninates was studied in collaboration with Dr. Alexander B. Sorokin (Institut de recherches sur la catalyse et l'environnement, Lyon, France).

Iron(III) phthalocyaninate decorated with crown ether substituents, [(15C5)$_4$PcFe]Cl, efficiently catalyzed the insertion of carbene derived from ethyl diazoacetate to six amines functionalized with thiazole, thiazoline and thiadiazole heterocycles. The reactions were carried out under practical conditions using EDA: amine stoichiometric ratio with 0.05 mol% catalyst loading.[37]

Electron-rich ruthenium phthalocyanine complexes were evaluated in carbene transfer reactions from ethyl diazoacetate (EDA) to aromatic and aliphatic olefins as well as to a wide range of aromatic, heterocyclic and aliphatic amines for the first time.[38] It was revealed that the ruthenium octabutoxyphthalocyanine carbonyl complex [(BuO)$_8$Pc]Ru(CO) is the most efficient catalyst converting electron-rich and electron-poor aromatic olefins to cyclopropane derivatives with high yields (typically 80–100%) and high TON (up to 1000) under low catalyst loading and nearly equimolar substrate/EDA ratio. This catalyst showed a rare efficiency in the carbene insertion into amine N–H bonds. Using a 0.05 mol% catalyst loading, a high amine concentration (1 M) and 1.1 eq. of EDA, a number of structurally divergent amines were selectively converted to mono-substituted glycine derivatives with up to quantitative yields and turnover numbers reaching 2000. High selectivity, large substrate scope, low catalyst loading and practical reaction conditions place [(BuO)$_8$Pc]Ru(CO) among the most efficient catalysts for the carbene insertion into amines.

Ruthenium phthalocyanine complexes bearing *n*-OBu substituents in the peripheral or non-peripheral positions were efficient catalysts for the selective double or single carbene insertion to the amine N–H bonds.[39] This complementary reactivity of two Ru complexes can be used for the synthesis of asymmetric tertiary amines and diamines bearing different substituents and has been demonstrated by two examples of readily available primary amines using different carbene precursors in successive reactions (Figure 12).

Novel ruthenium complexes have been synthesized for possible catalytic and photocatalytic applications. Series of substituted μ-carbido diruthenium(IV) bisphthalocyaninates was synthesized using two alternative approaches[40] – (i) direct metalation of phthalocyanines with $Ru_3(CO)_{12}$ in refluxing *o*-dichlorobenzene where [Pc*Ru]$_2$(μ-C) are formed as by-products together with monomeric complexes [Pc*Ru](CO) and (ii) dimerization of [Pc*Ru](CO) by dichlorocarbene generated in situ from chloroform and bases, which affords target complexes in high yield. Application of the appropriate base – NMe_4OH was found to be crucial in the case of synthesis of crown-substituted μ-carbido dimers.

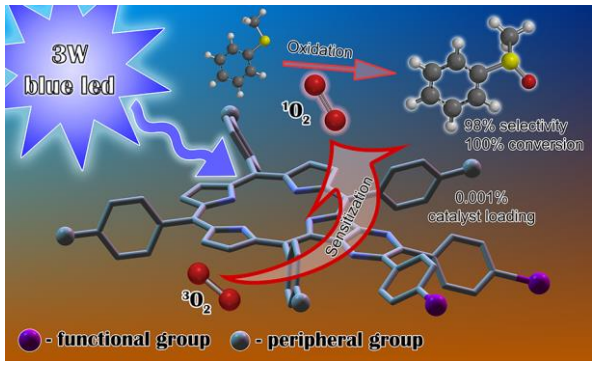

Figure 11. Diaryl-pyrazinoporphyrins – prospective photocatalysts for efficient sulfoxidation.[35]

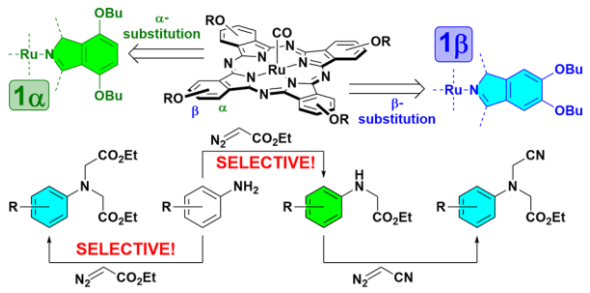

Figure 12. Substitution pattern in ruthenium octa-*n*-butoxyphthalocyanine complexes influence their reactivity in N–H carbene insertions.[39]

We also reported an extensive study of axial ligand replacement in ruthenium(II) complexes with tetra-tert-butyl-phthalocyanine (tBu$_4$Pc).[18] For this purpose oxidative decarbonylation of [tBu$_4$PcRu](CO) in the presence of trimethylamine was performed providing [tBu$_4$PcRu](NMe$_3$)$_2$. Its heating with pyrazine in *o*-dichlorobenzene at 100 °C gave [tBu$_4$PcRu](Pyz)$_2$ in quantitative yield. A simplified TD-DFT approximation has been used to explain the difference in the appearance of UV–Vis spectra of synthesized complexes with different N-donor ligands in terms of π-π* or charge transfer excitations, assignment was validated by the studies of solvatochromism of synthesized complexes. The reported finding can pave a convenient way to a relatively mild selective synthesis of ruthenium phthalocyaninates carrying N-donor aromatic ligands. Such complexes attract interest for various photo- and electroactive applications, catalysis and medicine.

Hybrid Materials

First examples of supramolecular hybrid organic–inorganic cluster-porphyrin systems constructed via metal–ligand coordination have been reported (with Prof. Sokolov group, NIIC, Novosibirsk).[41] The pyridine end-decorated Mo(II) halide cluster, possessing remarkable photophysical properties, was chosen as the inorganic part and zinc porphyrin was selected as the organic part. The crystal structures of hybrids bearing either two or six porphyrin units per one cluster were demonstrated (Figure 13).

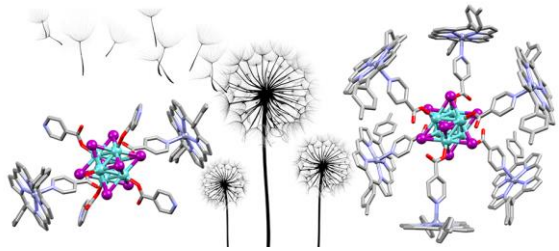

Figure 13. Hybrid organic–inorganic supramolecular systems based on a pyridine end-decorated molybdenum (II) halide cluster and zinc (II) porphyrinate.[41]

Porphyrin-based metal–organic frameworks on surfaces are a new class of planar materials with promising features for applications in chemical sensing, catalysis, and organic optoelectronics at nanoscale. We studied systematically a series of the SURMOFs assembled from *meso*-carboxyphenyl/pyridyl-substituted porphyrins and zinc acetate on template monolayers of graphene oxide via layer-by-layer deposition.[42] This microscopically flat template initiated the growth of macroscopically uniform SURMOF films exhibiting well-resolved X-ray diffraction. By applying the D'yakonov method, which has been previously used for the extraction of self-convolution of electron density in clay minerals, to the analysis of the experimental diffraction patterns of the SURMOFs, we determined the relation between the structure of porphyrin linkers and the geometry of packing motives in the films. Our method provides an enlightening picture of the interplay between supramolecular ordering and surface-directed assembly in porphyrin-based SURMOFs and is useful for rationalizing the fabrication of various classes of layered metal–organic frameworks on solids.

We studied the SAM-forming ability of a simple octylthiobenzoate and a redox-active metal-free phthalocyanine bearing two thiobenzoyl-terminated diethyleneglycol chains.[43] By the means of cyclic voltammetry for both solutions and SAMs of the studied phthalocyanine compound, it was demonstrated that this anchoring group does indeed allow formation of densely packed SAMs from the thiobenzoyl-containing compounds on gold surface without the need in additional ex situ deprotection synthetic step. This approach can be used for further design of novel building blocks for SAM containing this anchor group.

The post-modification of UiO-type materials with a porphyrin bearing phosphonic acid moieties is reported for the first time (Figure 14).[44] The prolonged interaction of UiO-66 and tetrakis(4-phosphonatophenyl)porphyrinato nickel(II) resulted in the formation of a hybrid material with the preservation of the crystallinity of the material. Thorough physical-chemical analysis of the obtained material and its precursors allowed assuming the binding motifs of the phosphonic acid residues.

The efficient application of the trialkylammonium group as an anchor for grafting of porphyrin to silica was demonstrated on the example of the novel imidazoporphyrin bearing peripheral triethylammonium unit.[45] The optimal synthetic sequence towards the target type of functional derivatives was revealed. The grafting of the prepared Ni(II) porphyrin to the surface of the commercially available silica was performed and the stability of the obtained hybrid material was investigated.

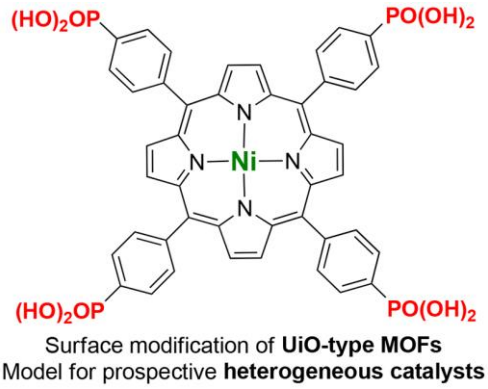

Figure 14. An approach towards modification of UiO-type MOFs with phosphonate-substituted porphyrins.[44]

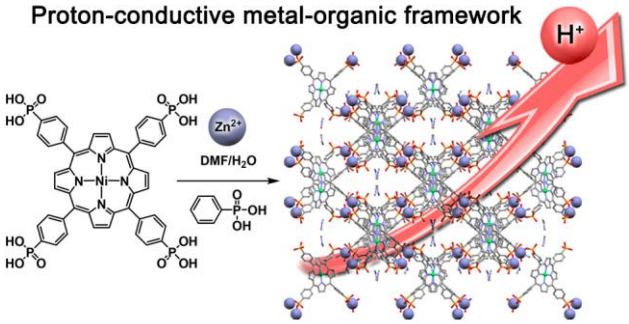

Figure 15. Highly proton-conductive zinc metal-organic framework based on nickel(II) porphyrinylphosphonate.[46]

Proton-Conducting Metal–Organic Frameworks

The design of new solid-state proton-conducting materials is a great challenge for chemistry and materials science. Thus, a new anionic porphyrinylphosphonate-based MOF (**IPCE-1Ni**), which involves dimethylammonium (DMA) cations for charge compensation, was reported (Figure 15).[46] As a result of its unique structure, **IPCE-1Ni** exhibited one of the highest values of the proton conductivity among reported proton-conducting MOF materials based on porphyrins ($1.55 \cdot 10^{-3}$ S·cm^{-1} at 75 °C and 80 % relative humidity). Studies of hydrogen conductivity were performed in collaboration with laboratory of ionics of functional materials (IGIC RAS).

A novel metal–organic framework **IPCE-2Ni** based on partially deprotonated 5,10,15,20-tetrakis(3-(phosphonatophenyl)-porphyrinato-nickel(II) species), with outstanding proton conductivity ($1.0 \cdot 10^{-2}$ S·cm^{-1} at 75 °C and 95 % relative humidity) has been obtained.[47] The high concentration of free phosphonate groups and compensating dimethylammonium cations bound by hydrogen bonds in the unique crystal structure of **IPCE-2Ni** is a key factor responsible for the observed high proton conductivity, which is one order of magnitude higher than for the MOF **IPCE-1Ni** and comparable with that of leaders among MOFs.

The synthesis and characterization of novel anionic Zn-containing MOF based on palladium(II) *meso*-tetrakis(3-

(phosphonatophenyl))porphyrinate, **IPCE-2Pd**, were reported (Figure 16).[48] Moreover, the proton-conductive properties and structures of two anionic Zn-containing MOFs based on nickel(II) and palladium(II) porphyrinylphosphonates, **IPCE-2M** (M = Ni(II) or Pd(II)), were compared in details. The high proton conductivity of $1.0 \cdot 10^{-2}$ S·cm^{-1} at 75 °C and 95% relative humidity (RH) is revealed for **IPCE-2Ni**, while **IPCE-2Pd** exhibits higher hydrolytic and thermal stability of the material (up to 420 °C) simultaneously maintaining a comparable value of conductivity ($8.11 \cdot 10^{-3}$ S·cm^{-1} at 95 °C and 95% RH). The nature of the porphyrin metal center is responsible for the features of crystal structure of materials, obtained under identical reaction conditions. The presence of phosphonic groups in compared materials **IPCE-2M** afforded a high concentration of proton carriers that together with the sorption of water molecules lead to a high proton conductivity.

Synthesis, structure, sorption properties and application prospects of porous porphyrin-based metal-organic frameworks were summarized in a comprehensive review.[49]

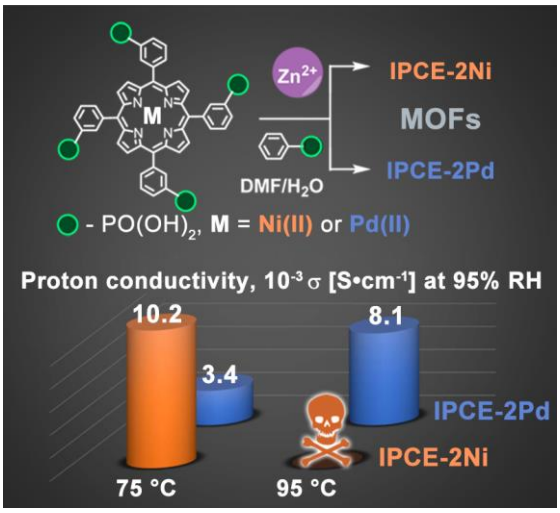

Figure 16. Proton conductivity as a function of the metal center in porphyrinylphosphonate-based MOFs.[48]

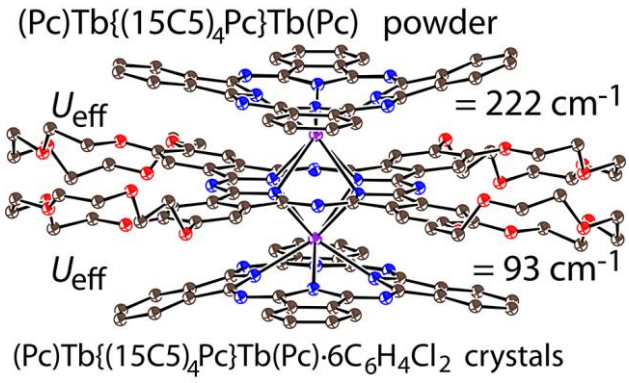

Figure 17. Single-molecule magnets based on heteroleptic terbium (III) trisphthalocyaninate in solvent-free and solvent-containing forms.[52]

Magnetic Materials

Magnetic properties of lanthanide complexes with phthalocyanine ligands provide them with various possible applications including single-molecule magnetism as well as NMR thermometry and tomography. Application of NMR as a versatile tool for studying the structure and magnetic properties of paramagnetic lanthanide complexes in solutions was summarized in 2021.[50]

In collaboration with Institute of Problems of Chemical Physics RAS we studied SMM behaviour of double-[51] and triple-decker[52] terbium(III) phthalocyaninates depending on their redox-state and solvation in crystalline phase (Figure 17).

Series of reports on NMR thermosensing properties of binuclear triple-decker complexes of lanthanides with 15-crown-5-phthalocyanine Ln[(15C5)$_4$Pc]$_3$ was reported[53–56] in collaboration with Nikolaev Institute of Inorganic Chemistry, The Siberian Branch of the Russian Academy of Sciences. Measuring the lanthanide-induced shift values for Tb(III) complex in $CDCl_3$ has revealed high temperature sensitivity for the signals of the aromatic protons of the inner deck: $\partial\delta/\partial T = 1.1$ ppm/K (Figure 18). It is the highest sensitivity of the LIS among the published complexes of 4f and d elements with polydentate ligands in organic media thus it can be considered as an NMR thermosensors in non-polar solutions. The possibility of the solubilization of complexes in aqueous media due to the presence of crown ether moieties has been also demonstrated.

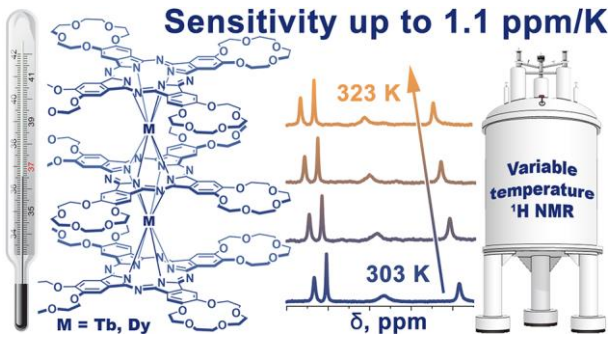

Figure 18. NMR thermosensing properties on binuclear triple-decker complexes of terbium(III) and dysprosium(III) with 15-crown-5-phthalocyanine.[53]

Original and efficient approach toward hydrophilization of Gd(III) complex with hydrophobic octabutoxyphthalocyanine was reported.[57] It consists in the solvent-mediated self-assembly of the preliminary synthesized octabutoxyphthalocyaninatogadolinium(III) acetate into the colloid species followed by their hydrophilization through the polyelectrolyte deposition. The magnetic behavior of the complex revealed it as pure paramagnetic, while magnetic relaxation behavior of the colloids pointed to some specificity. The r_2/r_1 ratio measured at 0.47 T is higher (2.6) than the ratios commonly reported for Gd(III) complexes, coming to 36.8 at 11.75 T. Thus, the synthesized colloids were more efficient as T_2- than T_1-contrasting agents at magnetic field strengths above 1.4 T.

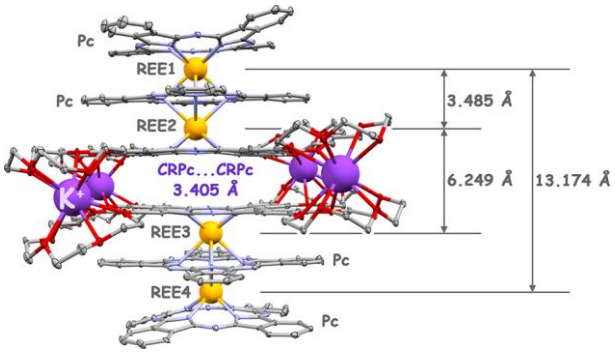

Figure 19. Cation-induced dimerization of heteroleptic crown-substituted trisphthalocyaninates as revealed by X-ray diffraction and NMR spectroscopy.[58]

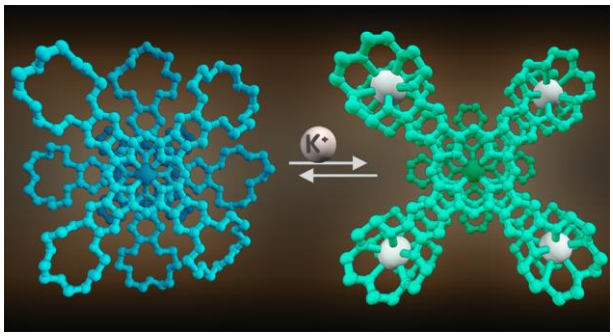

Figure 20. Heteroleptic crown-substituted tris(phthalocyaninates) as dynamic supramolecular scaffolds with switchable rotational states and tunable magnetic properties.[59]

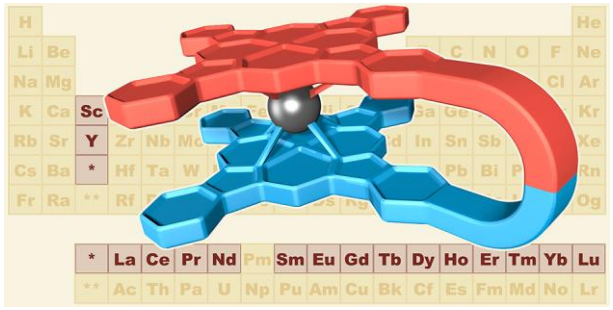

Figure 21. Rare-earth based tetrapyrrolic sandwiches: chemistry, materials and applications.[61]

Special attention was paid to sandwich phthalocyanine complexes with rare earth elements capable of supramolecular assembling. Thus, we firstly reported comprehensive X-ray diffraction and NMR studies of potassium-induced dimerization of heteroleptic triple-decker crown-phthalocyaninates [(15C5)$_4$Pc]M(Pc)M(Pc) (M = Y and Tb).[58] Characterization of the crystalline dimer gave the first structural evidence of the formation of a six-decker structure with four rare earth metal ions perfectly aligned near the symmetry axis (Figure 19). NMR studies of soluble supramolecular dimers provided a spectral–structural model that allowed us to assign the NMR spectra of related complexes with paramagnetic lanthanides and to further evaluate their structure and long-range interaction between the Ln(III) centers in multinuclear tetrapyrrolic complexes. The obtained results are promising for elaboration of new supramolecular magnetic materials.

In contrast to the other crown-substituted phthalocyanines, the interaction of K^+ cations with [(15C5)$_4$Pc]M*[(15C5)$_4$Pc]M(Pc) or [M*,M] did not induce their intermolecular aggregation.[59] Instead, the cations reversibly intercalate between the crown-substituted phthalocyanine ligands, resulting in switching of the coordination polyhedron of the metal center M* from square-antiprismatic to square-prismatic (Figure 20). In the case of terbium(III) complexes, such a switching altered their magnetic properties, which can be read-out by ^{1}H NMR spectroscopy. For [Tb*,Y], such a switching causes an almost 25% increase in the axial component of the magnetic susceptibility tensor. Even though the polyhedron of the paramagnetic center in [Y*,Tb] is not switched, minor structural perturbations associated with the overall reorganization of the receptor also cause smaller, but nevertheless appreciable, growth of the axial anisotropy. The observed effects render the studied complexes as molecular switches with tuneable magnetic properties.

We reported the comprehensive conformational study of substituted terbium(III) and yttrium(III) trisphthalocyaninates in solution depending on the substituents at the periphery of molecules, redox-states and nature of solvents.[60] Conjunction of UV-vis-NIR spectroscopy and quantum-chemical calculations within simplified time-dependent DFT in Tamm–Dancoff approximation provided the spectroscopic signatures of staggered and gauche conformations of trisphthalocyaninates. Altogether, it allowed us to demonstrate that the butoxy-substituted complex behaves as a molecular switcher with controllable conformational state, while the crown-substituted triple-decker complex maintains a staggered conformation regardless of external factors. The analysis of noncovalent interactions within the reduced density gradient approach allowed to shed light on the nature of factors stabilizing certain conformers.

Chemistry, materials and applications of rare-earth based tetrapyrrolic sandwiches was summarized in a comprehensive review (Figure 21).[61]

Molecular Switches and Supramolecular Chemistry

The Pt(II) and Pd(II) complexes were co-crystallized with highly electron-deficient arene systems to form reverse arene sandwich structures built by π-hole···[M^{II}] (d^{8}M=Pt, Pd) interactions (Figure 22).[62] The reverse sandwiches are based on noncovalent interactions and calculations indicate that in π-hole···[M^{II}] contacts, [M^{II}] plays the role of a nucleophile.

Reversible nucleophilic addition to a phthalocyanine core was observed for the first time for the electron-deficient cationic phosphorus(V) complex [PcP(OMe)$_2$]$^+$, whose reaction with KOH afforded a highly distorted nonaromatic adduct bearing an OH group at one of the α-pyrrolic carbon atoms (Figure 23).[19] This adduct was characterized by single-crystal X-ray diffraction, ESI HRMS, and NMR, and UV–vis spectroscopy, together with quantum-chemical modelling. The acidic treatment of this adduct restored aromaticity and recovered the starting cationic

complex. The reversible aromaticity breakage resulted in dramatic changes in the photophysical properties of the studied complex, which could pave the way to novel switchable Pc-based compounds and materials. Synthesis of P(V) phthalocyaninates with oxy/hydroxy axial ligands makes it possible to switch the photochemical and photophysical properties of complexes by reversible protonation/deprotonation.[21]

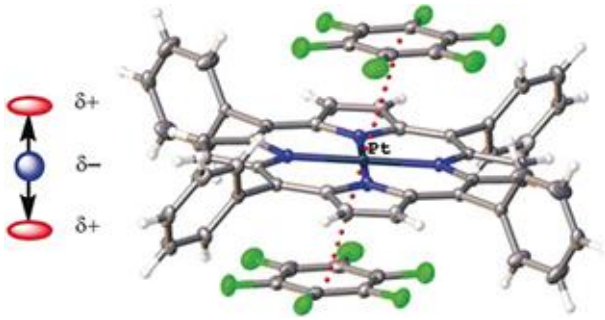

Figure 22. Reverse arene sandwich structures based upon π-Hole···[M^{II}] (d^8 M=Pt, Pd) interactions, where positively charged metal centers play the role of a nucleophile.[62]

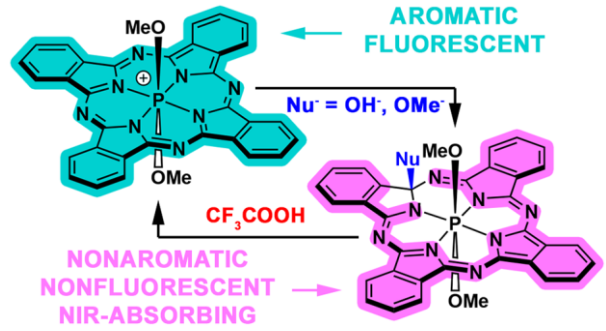

Figure 23. Switchable aromaticity of phthalocyanine via reversible nucleophilic aromatic addition to an electron-deficient phosphorus (V) complex.[19]

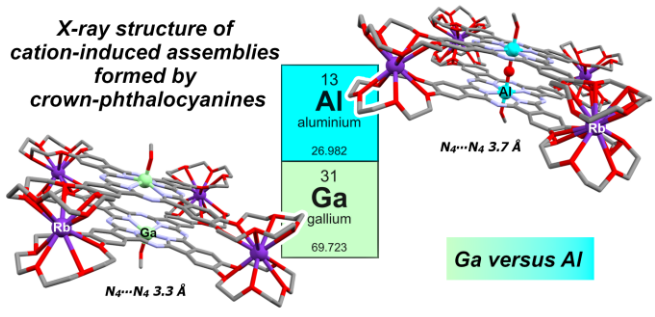

Figure 24. Cation-induced dimerization of crown-substituted gallium phthalocyanine by complexing with alkali metals: the crucial role of a central metal.[65]

Detection of nitroaromatic compounds (NAC) is an important task since these substances are hazardous to both the biosphere and the society. Fluorescent sensors developed for NAC detection usually demonstrate a 'turn-off' response to the analyte, while 'turn-on' sensors are rarely reported. We published a showcase report on new pyrene-imidazoporphyrin dyads that demonstrate an unusual analytic response to NAC with clear 'turn-on' behavior followed by an unexpected appearance of a new band, which can be ascribed to exciplex emission.[63] The porphyrin backbone of the dyad also allows registration of its own fluorescence, providing an internal reference signal for ratiometric detection.

Supramolecular assembling of crown-substituted phthalocyanines

Cation-induced supramolecular assembling of crown-substituted tetrapyrrole macrocycles is a powerful tool to obtain functional materials. A single-crystal X-ray diffraction study of a supramolecular dimer formed by [(15C5)$_4$Pc]Al(OH) with rubidium isonicotinate demonstrated that two molecules of the aluminum crown-phthalocyaninate isonicotinate are connected through an Al–O–Al bridge supported by sandwiching of crown ether moieties by Rb^+ cations.[64] No μ-oxo bridge was observed between the gallium atoms in the supramolecular dimers under similar conditions, despite the fact that aluminum and gallium belong to the same group of the Periodic table (Figure 24).[65]

A novel method exploiting the binding between crown-substituted double-decker phthalocyaninate Lu[(15C5)$_4$Pc]$_2$ and K^+ ions was applied for the one-step fabrication of macroscopically long conductive one-dimensional quasi-metal–organic frameworks.[66] It yielded fully conjugated intermolecular-bonded nanowires with a thickness of 10–50 nm, a length of up to 50 μm, and a conductivity of up to 11.4 S cm^{-1}, the highest among them being reported for phthalocyanine assemblies. A field-assisted method was developed to deposit aligned conductive assemblies on solids. The solid-supported nanowires can be disintegrated into starting components in a good aprotic solvent for further recycling (Figure 25).

Then we describe the method of planar organization of the aforementioned nanowires into ordered ultrathin films. The method utilized the Langmuir-Blodgett technique in combination with adding tert-butylamine during the synthesis of the supramolecular aggregates.[67] The atomic force microscopy examination of the resulting films showed that the introduction of surfactant promoted spreading of hydrophobic aggregates on the water subphase yielding ordered ultrathin layers. The proposed strategy can be used to obtain ordered coatings from 1D aggregates from various organic discotics with semiconductor properties.

Molecular switches at the interface

The ongoing collaboration with the Laboratory of physical chemistry of supramolecular systems IPCE RAS included studies of molecular switches at the air/water interface in Langmuir monolayers and on electroactive materials.

Achievement of information storage at molecular level remains a pressing task in miniaturization of computing technology. One of the promising approaches for its practi-

cal realization is development of nanoscale molecular switching materials including redox-active systems. The reported work demonstrated a concept of expansion of a number of available redox-states of self-assembled monolayers through supramolecular approach.[68] For this, we synthesized an octopus-like heteroleptic terbium(III) bisphthalocyaninate bearing one ligand with eight thioacetate-terminated "tentacles" (*octopus*-Pc) and a ligand with four crown-ether moieties (H_2[(15C5)$_4$Pc]). It is shown that *octopus*-Pc forms stable monolayers on gold, where its face-on orientation allows for subsequent binding of crown-phthalocyanine molecules via potassium ion bridges, which brings an additional redox-state to the system, thus expanding the multistability of the system as a whole (Figure 26). All four redox states available to this system exhibit characteristic absorbance in visible range, allowing for the switching to be easily read out using optical density measurements. The proposed approach can be used in wide range of switchable materials – single-molecule magnets, conductive, and optical devices, *etc*.

Redox isomerism, that is, the change of a metal cation valence state in organic complexes, can find promising applications in multistable molecular switches for various molecular electronic devices. However, despite a large number of studies devoted to such processes in organic complexes of multivalent lanthanides, redox-isomeric transformations were never observed for europium. We demonstrated the unique case of redox isomerization of Eu(III)/Eu(II) complexes on the example of Eu double-decker octa-*n*-butoxyphthalocyaninate (Eu[(BuO)$_8$Pc]$_2$) under ambient conditions (Figure 27).[69] Both redox-isomeric states were directly observed by X-ray absorption near-edge structure spectroscopy in ultrathin films formed under different conditions. Similar redox-switchable behavior was revealed for other Ln(II/III) complexes including Sm, Er, Tm and Yb.[70] Fluorescence mode XANES spectroscopy was found to be a powerful tool for redox-isomerism studies in ultrathin films.[71]

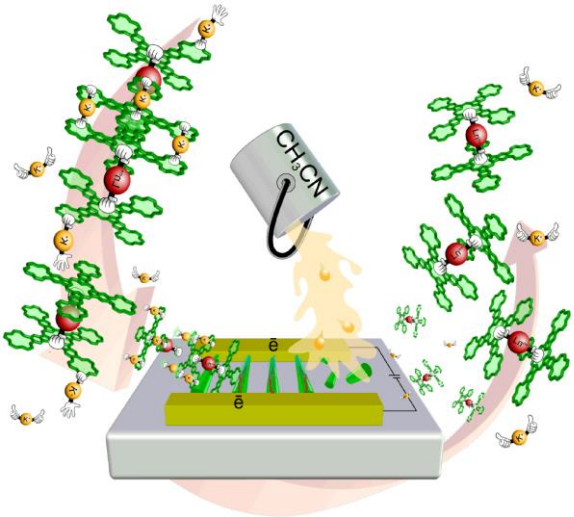

Figure 25. Ion-driven self-assembly of lanthanide bisphthalocyaninates into conductive quasi-MOF nanowires: an approach toward easily recyclable organic electronics.[66]

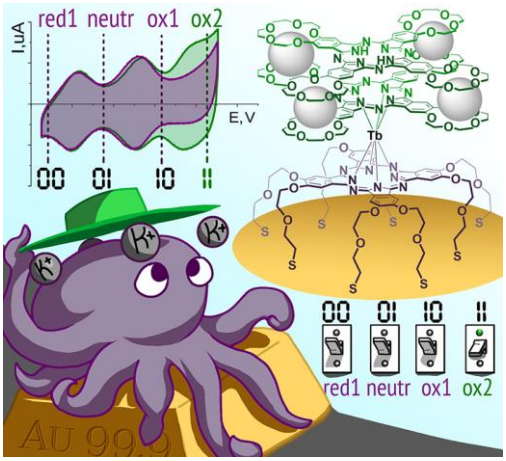

Figure 26. Octopus- type crown- bisphthalocyaninate anchor for bottom- up assembly of supramolecular bilayers with expanded redox- switching capability.[68]

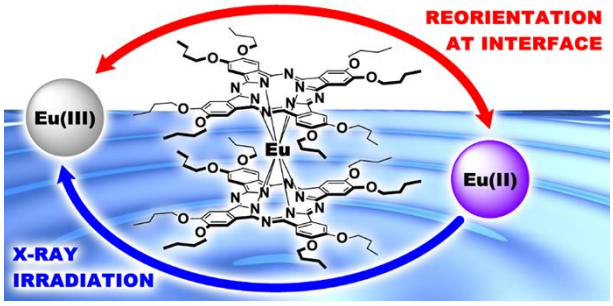

Figure 27. Long-sought redox isomerization of the europium(III/II) complex achieved by molecular reorientation at the interface.[69]

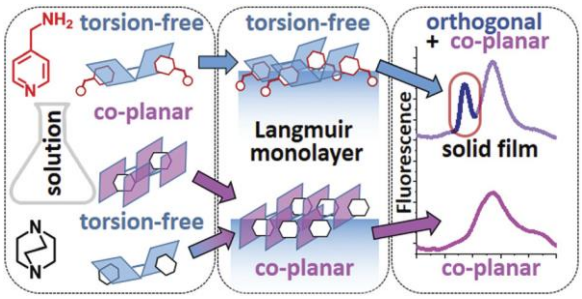

Figure 28. Restriction of the rotational relaxation of a butadiyne-bridged porphyrin dimer in ultrathin films.[73]

The dynamic behaviour of a porphyrin dimer, based on the covalent linkage of two macrocyclic moieties with a butadiyne connector, was studied in thin films by UV-Vis and emission spectroscopies.[72,73] By exploiting the propensity of the dimer to bind axial ligands through Zn–N bonds, it was shown that the co-planar and orthogonal conformations of the dimer may be stabilized in ultrathin films at the air/water interface (Figure 28). Furthermore, using the Langmuir–Blodgett technique, monolayer-thick matrix-free films on solid substrates containing the porphyrin dimer

were obtained. In the latter case, the dimer existed in either an exclusively co-planar state or a mixture of conformational states depending on the nature of the axial ligand: 1,4-diazabicyclo[2.2.2]-octane or 4-aminomethylpyridine. This work was performed in collaboration with Molecular Tectonics Laboratory, Université de Strasbourg, France.

We showed that coordination-induced spin crossover effect can be prompted for the commonly available nickel(II) tetraphenylporphyrinate, NiTPP, upon deposition of this complex at the air/water interface together with a ruthenium(II) phthalocyaninate, $[(15C5)_4Pc]]Ru(pyz)_2$, bearing two axial pyrazine ligands (Figure 29).[74] The latter was used as a molecular guiderail to align Ni···Ru···Ni metal centers for pyrazine coordination upon lateral compression of the system, which helps bring the two macrocycles closer together and forces the formation of Ni–pyz bonds. The fact of Ni(II) porphyrinate switching from low- to high-spin state upon acquiring additional ligands can be conveniently observed in situ via reflection-absorption UV-vis spectroscopy. The reversible nature of this interaction allows for dissociation of Ni–pyz bonds, and thus, change of nickel cation spin state, upon expansion of the monolayer.

Advances in elaboration of functional molecular switches involving tetrapyrrolic macrocycles were summarized in a comprehensive review (Figure 30).[75]

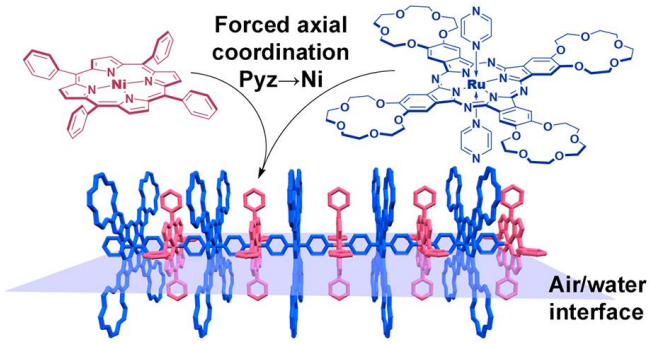

Figure 29. Spin crossover in nickel(II) tetraphenylporphyrinate via forced axial coordination at the air/water interface.[74]

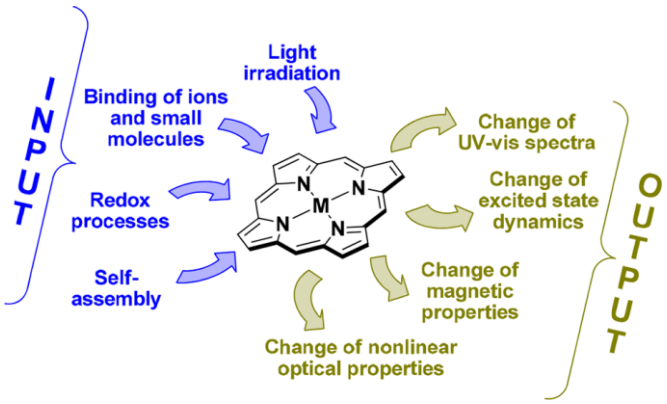

Figure 30. Functional molecular switches involving tetrapyrrolic macrocycles.[75]

References

1. Gorbunova Y.G., Martynov A.G., Stuzhin P.A., Koifman O.I. *Macroheterocycles* **2017**, *10*, 400–409. DOI: 10.6060/mhc171264g.
2. Birin K.P., Poddubnaya A.I., Abdulaeva I.A., Gorbunova Y.G., Tsivadze A.Y. *Dyes Pigm.* **2018**, *156*, 243–249. DOI:10.1016/j.dyepig.2018.04.009.
3. Abdulaeva I.A., Birin K.P., Gorbunova Y.G., Tsivadze A.Y., Bessmertnykh-Lemeune A. *J. Porphyrins Phthalocyanines* **2018**, *22*, 619–631. DOI:10.1142/S1088424618500475.
4. Abdulaeva I.A., Birin K.P., Polivanovskaia D.A., Gorbunova Y.G., Tsivadze A.Y. *RSC Adv.* **2020**, *10*, 42388–42399. DOI:10.1039/D0RA08603G.
5. Korobkov S.M., Birin K.P., Gorbunova Y.G., Tsivadze A.Y. *Dyes Pigm.* **2022**, *207*, 110696. DOI:10.1016/j.dyepig.2022.110696.
6. Birin K.P., Abdulaeva I.A., Poddubnaya A.I., Gorbunova Y.G., Tsivadze A.Y. *Dyes Pigm.* **2020**, *181*, 108550. DOI:10.1016/j.dyepig.2020.108550.
7. Abdulaeva I.A., Birin K.P., Sinelshchikova A.A., Grigoriev M.S., Lyssenko K.A., Gorbunova Y.G., Tsivadze A.Y., Bessmertnykh-Lemeune A. *CrystEngComm* **2019**, *21*, 1488–1498. DOI:10.1039/C8CE01992D.
8. Abdulaeva I.A., Polivanovskaia D.A., Birin K.P., Gorbunova Y.G., Tsivadze A.Y. *Mendeleev Commun.* **2020**, *30*, 162–164. DOI:10.1016/j.mencom.2020.03.010.
9. Abdulaeva I.A., Birin K.P., Bessmertnykh-Lemeune A., Tsivadze A.Y., Gorbunova Y.G. *Coord. Chem. Rev.* **2020**, *407*, 213108. DOI:10.1016/j.ccr.2019.213108.
10. Safonova E.A., Polovkova M.A., Martynov A.G., Gorbunova Y.G., Tsivadze A.Y. *Dalton Trans.* **2018**, *47*, 15226–15231. DOI:10.1039/C8DT03661F.
11. Martynov A.G., Berezhnoy G.S., Safonova E.A., Polovkova M.A., Gorbunova Y.G., Tsivadze A.Y. *Macroheterocycles* **2019**, *12*, 75–81. DOI:10.6060/mhc181225m.
12. Safonova E.A., Martynov A.G., Polovkova M.A., Ugolkova E.A., Minin V.V., Gorbunova Y.G., Tsivadze A.Y. *Dyes Pigm.* **2020**, *180*, 108484. DOI:10.1016/j.dyepig.2020.108484.
13. Yagodin A.V., Martynov A.G., Gorbunova Y.G., Tsivadze A.Y. *Dyes Pigm.* **2020**, *181*, 108564. DOI:10.1016/j.dyepig.2020.108564.
14. Yagodin A.V., Martynov A.G., Gorbunova Y.G., Tsivadze A.Y. *Macroheterocycles* **2021**, *14*, 130–134. DOI:10.6060/mhc210541m.
15. Martynov A.G., Mack J., May A.K., Nyokong T., Gorbunova Y.G., Tsivadze A.Y. *ACS Omega* **2019**, *4*, 7265–7284. DOI:10.1021/acsomega.8b03500.
16. May A., Majumdar P., Martynov A.G., Lapkina L.A., Troyanov S.I., Gorbunova Y.G., Tsivadze A.Y., Mack J., Nyokong T. *J. Porphyrins Phthalocyanines* **2020**, *24*, 589–601. DOI:10.1142/S108842462050011X.
17. Bunin D.A., Ndebele N., Martynov A.G., Mack J., Gorbunova Y.G., Nyokong T. *Molecules* **2022**, *27*, 524. DOI:10.3390/molecules27020524.
18. Dmitrienko A.A., Kroitor A.P., Demina L.I., Gorbunova Y.G., Sorokin A.B., Martynov A.G. *Polyhedron* **2022**, *220*, 115821. DOI:10.1016/j.poly.2022.115821.
19. Kolomeychuk F.M., Safonova E.A., Polovkova M.A., Sinelshchikova A.A., Martynov A.G., Shokurov A.V., Kirakosyan G.A., Efimov N.N., Tsivadze A.Y., Gorbunova Y.G. *J. Am. Chem. Soc.* **2021**, *143*, 14053–14058. DOI:10.1021/jacs.1c05831.
20. Meshkov I.N., Martynov A.G., Tsivadze A.Y., Gorbunova Y.G. *Macroheterocycles* **2019**, *12*, 143–147. DOI:10.6060/mhc190233m.
21. Safonova E., Kolomeychuk F., Gvozdev D., Tsivadze A., Gorbunova Y. *Molecules* **2023**, *28*, 1094. DOI:10.3390/molecules28031094.

22. Birin K.P., Gorbunova Y.G., Tsivadze A.Y. *Macroheterocycles* **2018**, *11*, 150–154. DOI:10.6060/mhc180280b.
23. Managa M., Khene S., Britton J., Martynov A.G., Gorbunova Y.G., Tsivadze A.Y., Nyokong T. *J. Porphyrins Phthalocyanines* **2018**, *22*, 137–148. DOI:10.1142/S1088424618500128.
24. Birin K.P., Abdulaeva I.A., Polivanovskaia D.A., Martynov A.G., Shokurov A.V., Gorbunova Y.G., Tsivadze A.Y. *Dyes Pigm.* **2021**, *186*, 109042. DOI:10.1016/j.dyepig.2020.109042.
25. Kozhina E., Bedin S., Martynov A., Andreev S., Piryazev A., Grigoriev Y., Gorbunova Y., Naumov A. *Biosensors* **2023**, *13*, 46. DOI:10.3390/bios13010046.
26. Bunin D.A., Martynov A.G., Safonova E.A., Tsivadze A.Y., Gorbunova Y.G. *Dyes Pigm.* **2022**, *207*, 110768. DOI:10.1016/j.dyepig.2022.110768.
27. Kolesnikov I.E., Kurochkin M.A., Meshkov I.N., Akasov R.A., Kalinichev A.A., Kolesnikov E.Y., Gorbunova Y.G., Lähderanta E. *Mater. Des.* **2021**, *203*, 109613. DOI:10.1016/j.matdes.2021.109613.
28. Kolesnikov I.E., Kalinichev A.A., Solomatina A.I., Kurochkin M.A., Meshkov I.N., Kolesnikov E.Y., Gorbunova Y.G. *Sensors Actuators A Phys.* **2022**, *347*, 113917. DOI: 10.1016/j.sna.2022.113917.
29. Volostnykh M.V., Borisov S.M., Konovalov M.A., Sinelshchikova A.A., Gorbunova Y.G., Tsivadze A.Y., Meyer M., Stern C., Bessmertnykh-Lemeune A. *Dalton Trans.* **2019**, *48*, 8882–8898. DOI:10.1039/C9DT01577A.
30. Sokolov V.S., Batishchev O.V., Akimov S.A., Galimzyanov T.R., Konstantinova A.N., Malingriaux E., Gorbunova Y.G., Knyazev D.G., Pohl P. *Sci. Rep.* **2018**, *8*, 14000. DOI:10.1038/s41598-018-31901-9.
31. Jiménez-Munguía I., Fedorov A.K., Abdulaeva I.A., Birin K.P., Ermakov Y.A., Batishchev O.V., Gorbunova Y.G., Sokolov V.S. *Biomolecules* **2019**, *9*, 853. DOI:10.3390/biom9120853.
32. Polivanovskaia D.A., Konstantinova A.N., Birin K.P., Sokolov V.S., Batishchev O.V., Gorbunova Y.G. *Membranes (Basel)* **2022**, *12*, 846. DOI:10.3390/membranes12090846.
33. Shekunova T.O., Lapkina L.A., Shcherbakov A.B., Meshkov I.N., Ivanov V.K., Tsivadze A.Y., Gorbunova Y.G. *J. Photochem. Photobiol. A Chem.* **2019**, *382*, 111925. DOI:10.1016/j.jphotochem.2019.111925.
34. Teplonogova M.A., Volostnykh M.V., Yapryntsev A.D., Sozarukova M.M., Gorbunova Y.G., Sheichenko E.D., Baranchikov A.E., Ivanov V.K. *Int. J. Mol. Sci.* **2022**, *23*, 15373. DOI:10.3390/ijms232315373.
35. Polivanovskaia D.A., Abdulaeva I.A., Birin K.P., Gorbunova Y.G., Tsivadze A.Y. *J. Catal.* **2022**, *413*, 342–352. DOI:10.1016/j.jcat.2022.06.046.
36. Shremzer E.S., Polivanovskaia D.A., Birin K.P., Gorbunova Y.G., Tsivadze A.Y. *Dyes Pigm.* **2023**, *210*, 110935. DOI:10.1016/j.dyepig.2022.110935.
37. Cailler L.P., Martynov A.G., Gorbunova Y.G., Tsivadze A.Y., Sorokin A.B. *J. Porphyrins Phthalocyanines* **2019**, *23*, 497–506. DOI:10.1142/S1088424619500354.
38. Cailler L.P., Kroitor A.P., Martynov A.G., Gorbunova Y.G., Sorokin A.B. *Dalton Trans.* **2021**, *50*, 2023–2031. DOI:10.1039/D0DT04090H.
39. Kroitor A.P., Dmitrienko A.A., Martynov A.G., Gorbunova Y.G., Sorokin A.B. *Org. Biomol. Chem.* **2023**, *21*, 69–74. DOI:10.1039/D2OB01861F.
40. Kroitor A.P., Martynov A.G., Gorbunova Y.G., Tsivadze A.Y., Sorokin A.B. *Eur. J. Inorg. Chem.* **2019**, *2019*, 1923–1931. DOI:10.1002/ejic.201900029.
41. Volostnykh M.V., Mikhaylov M.A., Sinelshchikova A.A., Kirakosyan G.A., Martynov A.G., Grigoriev M.S., Piryazev D.A., Tsivadze A.Y., Sokolov M.N., Gorbunova Y.G. *Dalton Trans.* **2019**, *48*, 1835–1842. DOI:10.1039/C8DT04452J.
42. Meshkov I.N., Zvyagina A.I., Shiryaev A.A., Nickolsky M.S., Baranchikov A.E., Ezhov A.A., Nugmanova A.G., Enakieva Y.Y., Gorbunova Y.G., Arslanov V.V., Kalinina M.A. *Langmuir* **2018**, *34*, 5184–5192. DOI:10.1021/acs.langmuir.7b04384.
43. Shokurov A.V., Yagodin A.V., Martynov A.G., Gorbunova Y.G., Selektor S.L. *ECS J. Solid State Sci. Technol.* **2020**, *9*, 051006. DOI:10.1149/2162-8777/ab9a5e.
44. Birin K.P., Shlykov I.V., Senchikhin I.N., Demina L.I., Gorbunova Y.G., Tsivadze A.Y. *Polyhedron* **2022**, *219*, 115794. DOI:10.1016/j.poly.2022.115794.
45. Nikulin V.O., Birin K.P., Gorbunova Y.G., Tsivadze A.Y. *Macroheterocycles* **2021**, *14*, 323–327. DOI:10.6060/mhc224231b.
46. Enakieva Y.Y., Sinelshchikova A.A., Grigoriev M.S., Chernyshev V.V., Kovalenko K.A., Stenina I.A., Yaroslavtsev A.B., Gorbunova Y.G., Tsivadze A.Y. *Chem. – A Eur. J.* **2019**, *25*, 10552–10556. DOI:10.1002/chem.201902212.
47. Enakieva Y.Y., Sinelshchikova A.A., Grigoriev M.S., Chernyshev V.V., Kovalenko K.A., Stenina I.A., Yaroslavtsev A.B., Gorbunova Y.G., Tsivadze A.Y. *Chem. – A Eur. J.* **2021**, *27*, 1598–1602. DOI:10.1002/chem.202003893.
48. Enakieva Y.Y., Zhigileva E.A., Fitch A.N., Chernyshev V.V., Stenina I.A., Yaroslavtsev A.B., Sinelshchikova A.A., Kovalenko K.A., Gorbunova Y.G., Tsivadze A.Y. *Dalton Trans.* **2021**, *50*, 6549–6560. DOI:10.1039/d1dt00612f.
49. Gorbunova Y.G., Enakieva Y.Y., Volostnykh M.V., Sinelshchikova A.A., Abdulaeva I.A., Birin K.P., Tsivadze A.Y. *Russ. Chem. Rev.* **2022**, *91*, 5038. DOI:10.1070/rcr5038.
50. Gorbunova Y.G., Martynov A.G., Birin K. P., Tsivadze A. Y., *Russ. J. Inorg. Chem.*, **2021**, *66*, 202–216. DOI:10.1134/S0036023621020091.
51. Konarev D.V., Khasanov S.S., Batov M.S., Martynov A.G., Nefedova I.V., Gorbunova Y.G., Otsuka A., Yamochi H., Kitagawa H., Lyubovskaya R.N. *Inorg. Chem.* **2019**, *58*, 5058–5068. DOI:10.1021/acs.inorgchem.9b00131.
52. Faraonov M.A., Martynov A.G., Polovkova M.A., Khasanov S.S., Gorbunova Y.G., Tsivadze A.Y., Otsuka A., Yamochi H., Kitagawa H., Konarev D.V. *Magnetochemistry* **2023**, *9*, 36. DOI:10.3390/magnetochemistry9020036.
53. Babailov S.P., Polovkova M.A., Kirakosyan G.A., Martynov A.G., Zapolotsky E.N., Gorbunova Y.G. *Sensors Actuators, A Phys.* **2021**, *331*, 112933. DOI:10.1016/j.sna.2021.112933.
54. Babailov S.P., Polovkova M.A., Zapolotsky E.N., Kirakosyan G.A., Martynov A.G., Gorbunova Y.G. *J. Porphyrins Phthalocyanines* **2022**, *26*, 334–339. DOI:10.1142/S1088424622500201.
55. Martynov A.G., Polovkova M.A., Kirakosyan G.A., Zapolotsky E.N., Babailov S.P., Gorbunova Y.G. *Polyhedron* **2022**, *219*, 115792. DOI:10.1016/j.poly.2022.115792.
56. Babailov S.P., Zapolotsky E.N., Fomin E.S., Polovkova M.A., Kirakosyan G.A., Martynov A.G., Gorbunova Y.G. *Molecules* **2022**, *27*, 7836. DOI:10.3390/molecules27227836.
57. Zairov R.R., Yagodin A.V., Khrizanforov M., Martynov A.G., Nizameev I.R., Syakaev V.V., Gubaidullin A.T., Kornev T., Kaman O., Budnikova Y.H., Gorbunova Y.G., Mustafina A.R. *J. Nanoparticle Res.* **2019**, *21*, 12. DOI:10.1007/s11051-018-4455-4.
58. Martynov A.G., Polovkova M.A., Berezhnoy G.S., Sinelshchikova A.A., Dolgushin F.M., Birin K.P., Kirakosyan G.A., Gorbunova Y.G., Tsivadze A.Y. *Inorg. Chem.* **2020**, *59*, 9424–9433. DOI:10.1021/acs.inorgchem.0c01346.
59. Martynov A.G., Polovkova M.A., Berezhnoy G.S., Sinelshchikova A.A., Khrustalev V.N., Birin K.P., Kirakosyan G.A., Gorbunova Y.G., Tsivadze A.Y. *Inorg. Chem.* **2021**, *60*, 9110–9121. DOI:10.1021/acs.inorgchem.1c01100.
60. Martynov A.G., Polovkova M.A., Gorbunova Y.G., Tsivadze A.Y. *Molecules* **2022**, *27*, 6498. DOI:10.3390/molecules27196498.
61. Martynov A.G., Horii Y., Katoh K., Bian Y., Jiang J., Yamashita M., Gorbunova Y.G. *Chem. Soc. Rev.* **2022**, *51*, 9262–9339. DOI:10.1039/d2cs00559j.
62. Rozhkov A.V., Krykova M.A., Ivanov D.M., Novikov A.S., Sinelshchikova A.A., Volostnykh M.V., Konovalov M.A., Grigoriev M.S., Gorbunova Y.G., Kukushkin V.Y. *Angew. Chem. Int. Ed.* **2019**, *58*, 4164–4168. DOI:10.1002/anie.201814062.

63. Shepeleva I.I., Birin K.P., Polivanovskaia D.A., Martynov A.G., Shokurov A.V., Tsivadze A.Y., Selektor S.L., Gorbunova Y.G. *Chemosensors* **2023**, *11*, 43. DOI:10.3390/chemosensors11010043.
64. Lapkina L. A., Larchenko V. E., Kirakosyan G. A., Tsivadze A. Y., Troyanov S. I., Gorbunova Y. G., *Inorg. Chem.*, **2018**, 57, 82–85. DOI:10.1021/acs.inorgchem.7b01983.
65. Lapkina L.A., Sinelshchikova A.A., Birin K.P., Larchenko V.E., Grigoriev M.S., Tsivadze A.Y., Gorbunova Y.G. *Inorg. Chem.* **2021**, *60*, 1948–1956. DOI:10.1021/acs.inorgchem.0c03408.
66. Zvyagina A.I., Aleksandrov A.E., Martynov A.G., Tameev A.R., Baranchikov A.E., Ezhov A.A., Gorbunova Y.G., Kalinina M.A. *Inorg. Chem.* **2021**, *60*, 15509–15518. DOI:10.1021/acs.inorgchem.1c02147.
67. Zvyagina A.I., Naumova A.D., Kuzmina N.V., Martynov A.G., Gorbunova Y.G., Kalinina M.A. *Macroheterocycles* **2021**, *14*, 59–64. DOI:10.6060/mhc210233k.
68. Shokurov A.V., Yagodin A.V., Martynov A.G., Gorbunova Y.G., Tsivadze A.Y., Selektor S.L. *Small* **2022**, *18*, 2104306. DOI:10.1002/smll.202104306.
69. Shokurov A.V., Kutsybala D.S., Martynov A.G., Bakirov A.V., Shcherbina M.A., Chvalun S.N., Gorbunova Y.G., Tsivadze A.Y., Zaytseva A.V., Novikov D., Arslanov V.V., Selektor S.L. *Langmuir* **2020**, *36*, 1423–1429. DOI:10.1021/acs.langmuir.9b03403.
70. Kutsybala D.S., Shokurov A.V., Martynov A.G., Yagodin A.V., Arslanov V.V., Gorbunova Y.G., Selektor S.L. *Symmetry (Basel)* **2022**, *14*, 340. DOI:10.3390/sym14020340.
71. Shokurov A.V., Kutsybala D.S., Martynov A.G., Yagodin A.V., Gorbunova Y.G., Novikov D., Bakirov A.V., Shcherbina M.A., Chvalun S.N., Arslanov V.V., Selektor S.L. *Macroheterocycles* **2019**, *12*, 264–267. DOI:10.6060/mhc191071s.
72. Meshkov I.N., Bulach V., Gorbunova Y.G., Jouaiti A., Sinelshchikova A.A., Kyritsakas N., Grigoriev M.S., Tsivadze A.Y., Hosseini M.W. *New J. Chem.* **2018**, *42*, 7816–7822. DOI:10.1039/c8nj01219a.
73. Shokurov A. V., Meshkov I. N., Bulach V., Gorbunova Y. G., Hosseini M. W., Tsivadze A. Y., Arslanov V. V., Selektor S. L., *New J. Chem.*, **2019**, 43, 11419–11425. DOI:10.1039/c9nj01807g.
74. Shokurov A.V., Kutsybala D.S., Kroitor A.P., Dmitrienko A.A., Martynov A.G., Enakieva Y.Y., Tsivadze A.Y., Selektor S.L., Gorbunova Y.G. *Molecules* **2021**, *26*, 4155. DOI:10.3390/molecules26144155.
75. Martynov A.G., Safonova E.A., Tsivadze A.Y., Gorbunova Y.G. *Coord. Chem. Rev.* **2019**, *387*, 325–347. DOI:10.1016/j.ccr.2019.02.004.

Received 10.02.2023
Accepted 20.02.2023